Original Article
Yonsei Med J 2018 Aug;59(6):736-745
https://doi.org/10.3349/ymj.2018.59.6.736
Yonsei Medical Journal
YMJ
pISSN: 0513-5796 · eISSN: 1976-2437

Extracellular Vesicles Derived from Hypoxic Human Mesenchymal Stem Cells Attenuate GSK3β Expression via miRNA-26a in an Ischemia-Reperfusion Injury Model

Hyewon Park[1], Hyelim Park[1,2], Dasom Mun[1], Jiyoung Kang[1], Hyoeun Kim[1], Michael Kim[3], Shanyu Cui[1], Seung-Hyun Lee[2,4], and Boyoung Joung[1,2]

[1]Division of Cardiology, Yonsei University College of Medicine, Seoul, Korea;
[2]Brain Korea 21 PLUS Project for Medical Science, Yonsei University, Seoul, Korea;
[3]Department of Biomedical Engineering, Duke University, Durham, North Carolina, USA;
[4]Department of Biochemistry and Molecular Biology, Yonsei University College of Medicine, Seoul, Korea.

Purpose: Bioactive molecules critical to intracellular signaling are contained in extracellular vesicles (EVs) and have cardioprotective effects in ischemia/reperfusion (IR) injured hearts. This study investigated the mechanism of the cardioprotective effects of EVs derived from hypoxia-preconditioned human mesenchymal stem cells (MSCs).

Materials and Methods: EV solutions (0.4 μg/μL) derived from normoxia-preconditioned MSCs (EV_{NM}) and hypoxia-preconditioned MSCs (EV_{HM}) were delivered in a rat IR injury model. Successful EV delivery was confirmed by the detection of PKH26 staining in hearts from EV-treated rats.

Results: EV_{HM} significantly reduced infarct size (24±2% vs. 8±1%, p<0.001), and diminished arrhythmias by recovering electrical conduction, I_{Na} current, and Cx43 expression. EV_{HM} also reversed reductions in Wnt1 and β-catenin levels and increases in GSK3β induced after IR injury. miRNA-26a was significantly increased in EV_{HM}, compared with EV_{NM}, in real-time PCR. Finally, in *in vitro* experiments, hypoxia-induced increases in GSK3β expression were significantly reduced by the overexpression of miRNA-26a.

Conclusion: EV_{HM} reduced IR injury by suppressing GSK3β expression via miRNA-26a and increased Cx43 expression. These findings suggest that the beneficial effect of EV_{HM} is related with Wnt signaling pathway.

Key Words: Extracellular vesicles, ischemia reperfusion, arrhythmia, GSK3β, miRNA-26a

INTRODUCTION

The main goals in patients with acute myocardial infarction are to minimize myocardial damage, enhance cardiac repair, and decrease myocardial remodeling. Current high-tech therapy involves speedy reperfusion of the infarcted myocardium through revascularization of the occluded vessel. However, the advantage of reperfusion is compromised by the endothelial damage and inflammation that follow the reinstitution of the blood flow, leading to additional myocardial damage in a process named "ischemia/reperfusion (IR) injury."[1-3] IR injury can be accompanied by lethal ventricular arrhythmias in addition to the myocardial injury.

Mesenchymal stem cells (MSCs), and other cell types, release extracellular vesicles (EVs) that play a role in intercellular communication by transporting mRNA, microRNA, and proteins between cells. EVs are a class of membrane-bound organelles secreted by various cell types.[4] The potential for EVs

Received: March 20, 2018 **Revised:** May 4, 2018
Accepted: May 13, 2018
Corresponding author: Boyoung Joung, MD, PhD, Division of Cardiology, Yonsei University College of Medicine, 50-1 Yonsei-ro, Seodaemun-gu, Seoul 03722, Korea. Tel: 82-2-2228-8460, Fax: 82-2-393-2041, E-mail: cby6908@yuhs.ac

•The authors have no financial conflicts of interest.

to be used as therapeutic agents, or as biomarkers of pathological states, has generated enormous interest.[5,6] EVs have been implicated in the process of a remarkable antitumor effect in cancer by ameliorating tumor immune suppression, metastasis, and angiogenesis, along with having a primary role in tissue regeneration.[7-9] EVs have been proposed to stimulate favorable signaling pathways in cardiovascular disease: for example, potentially mediating the proangiogenic actions of human stem cells.[10] Studies have reported that the beneficial activity of the conditioned medium from MSCs is attributable to EVs.[11,12] Importantly, exposure to various stressors can change the composition of EVs to change the surrounding microenvironment through EV-mediated cell-to-cell communication.[13] In normal cell physiology, EV secretion is a protective process to eliminate harmful components released during harmful conditions, such as IR injury.[14] Under hypoxic conditions, genetically modified bone marrow-derived MSCs overexpressing *Akt1* have been found to release paracrine factors that exert cytoprotective effects on cardiomyocytes exposed to hypoxia.[15] Another study of the helpful byproduct effects of MSCs reported the release of cytokines from bone marrow stem cells boosting new vessel formation, inhibiting cardiomyocyte apoptosis, and maintaining myocardial contractility.[16] Recently, it was reported that MSC-derived exosomes increase ATP levels, decrease oxidative stress, activate the PI3K/Akt pathway, and increase phosphorylated-GSK3β levels to enhance myocardial viability and to prevent adverse remodeling after myocardial IR injury.[17]

Because GSK3β is associated with the Wnt-Fizzled pathway, we hypothesized that MSC-derived exosomes would attenuate IR injury by effecting Wnt pathways. To prove this hypothesis, we investigated whether EVs derived from MSCs cultured in hypoxic media (EV_{HM}) influence Wnt1, GSK3β, and β catenin. We also compared Wnt-related miRNA levels between EV_{HM} and EVs derived from MSCs cultured in normoxic media (EV_{NM}), and found significant increases in miRNA (miR) 26a in EV_{HM}. Finally, we demonstrated that EV_{HM} directly targets GSK3β using anti-miR-26a.

MATERIALS AND METHODS

This investigation conformed to the Guide for the Care and Use of Laboratory Animals published by the US National Institutes of Health, and was approved by the animal ethics committee of Yonsei University College of Medicine and Cardiovascular Research Institute (approval reference number 2016-0135).

Study groups

To establish an IR injury model, all adult male Sprague-Dawley rats (230±10 g) were anesthetized by intramuscular injection of ketamine hydrochloride (80 mg/kg) and xylazine hydrochloride (4 mg/kg). The rats were intubated, and were ventilated with positive pressure (180 mL/min) using a ventilator (Harvard Apparatus model 683, Millis, MA, USA). The small incision was operated at the left lateral costal rib to expose the heart. The left anterior descending artery was ligated for 1 h with a 6-0 silk suture (Ethicon, Somerville, NJ, USA), followed by reperfusion for 3 h. Immediately after the initiation of reperfusion, 125 μL of an EV solution (0.4 μg/μL) in phosphate buffered saline (PBS) (IR+EV_{NM} or IR+EV_{HM} group) or PBS alone (IR group) was systemically injected via the leg veins of the rats. We used sham-operated rats as controls. The animals were sacrificed 3 hours after the EV injection.

To measure the myocardial infarcted size, hearts were sectioned and incubated in 1% 2,3,5-triphenyltetrazolium chloride (TTC; Sigma-Aldrich, St Louis, MO, USA) for 30 min at 37°C. Each heart specimen was fixed for 24 h in 10% paraformaldehyde. Myocardium was identified as red, whereas infarcted areas appeared yellow. The region of normal and infarcted left ventricular myocardium was directly assessed by planimetry using dedicated software (ImageJ software, NIH software).

Immunohistochemical staining

For immunostaining of heart tissue, the anterior walls of the left ventricles were harvested after being fixed with 10% formaldehyde in PBS (pH 7.4), embedded with paraffin, and then sectioned at a thickness at 4 μm. Immunostaining was detected with the avidin-biotin complex (ABC) method. The primary antibodies used were rabbit anti-Cx43 polyclonal antibody (1:2000, Santa Cruz Biotechnology, Santa Cruz, CA, USA) detecting only Cx43. To inactive tissue endogenous peroxidase was then blocked by incubation with peroxidase block for 30 min, and then, the tissue sections were incubated for enzymatic retrieval, followed by 10% blocking serum. The slides were incubated overnight at room temperature, immunohistochemistry was colored using the polymer method (Vectastain ABC kits, PK-4000, Vector Laboratories, Burlingame, CA, USA), and later color development was performed with diaminobenzidine (DAB) and contrast staining with hematoxylin.

Western blotting

Rat heart samples were homogenized and centrifuged at 15000×g for 15 min at 4°C, and protein concentration was determined using the Pierce BCA Protein Assay kit (Thermo Scientific Inc., Rockford, IL, USA). The protein samples were separated using SDS-polyacrylamide gel, and the separated proteins were transferred to a nitrocellulose membrane (Bio-Rad, Richmond, CA, USA). After blocking with 10% non-fat milk/TBS-T for 1 h, the membrane was incubated with indicated primary antibodies [anti-CD81, HSP70, CD63 (System Biosciences, Palo Alto, CA, USA), Annexin, Integrin (Abcam, Cambridge, MA, USA), Wnt1, GSK3β, p-GSK3β, β-catenin, p-β-catenin (Cell Signaling, Danvers, MA, USA), Cx43 (Santa Cruz Biotechnology), and GAPDH (at a dilution of 1:1000, Cell Signaling) overnight at 4°C, and then incubated with horseradish peroxidase-conjugated sec-

ondary antibodies for 1h at room temperature. Western blot signals were assayed using a reinforced chemiluminescence detection system (ECL, Amersham Pharmacia Biotech, Piscataway, NJ, USA).[18]

Real-time polymerase chain reaction

A total of 500 ng RNA was extracted using TRIzol® Reagent (Invitrogen, Carlsbad, CA, USA) according to the manufacturer's instructions. cDNA was synthesized using a RevertAid™ First Strand cDNA Synthesis Kit (Fermentas, Ontario, Canada). Quantitative RT-PCR (qRT-PCR) was performed using SYBR® Premix Ex Taq™ II (TaKaRa, Otsu, Japan) for quantification. Triplicates were tested for each sample. The expression of the target miRNA were normalized by U6 snRNA, respectively. Purity of PCR products was identified using a melting curve.

miR and anti-miRNA transfection

We used four intended miRNA target prediction algorithms: DIANA-microT3.1, MirTarget2, miRDB, and TargetScan5.1. Conserved miRNAs that are expected to target a given gene in at least three of the four algorithms were considered as candidates for further analysis (Supplementary Figs. 1 and 2, only online).

miR targeting GSK3β and miR-26a-specific anti-miRNA were transfected into H9C2 cells using Lipofectamine RNAiMax

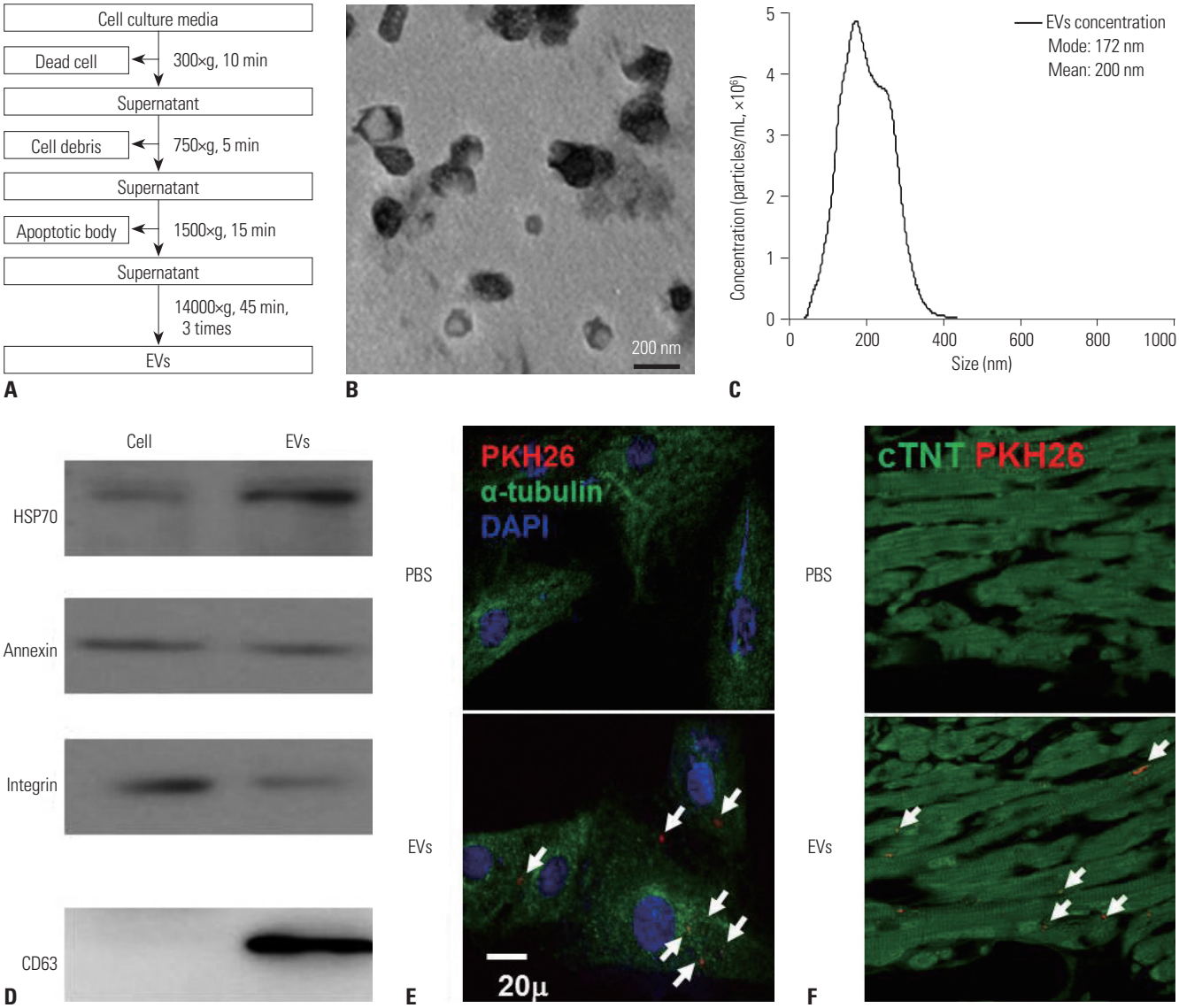

Fig. 1. Isolation, characterization, and delivery of EVs. (A) Isolation of EV-rich fractions from human MSC media using a standard protocol of serial differential centrifugation and ultracentrifugation steps. (B) Transmission electron microscopy image showing typical EVs. (C) Nanoparticle tracking analysis of EVs showing the number and size distributions of particles. (D) Western blot of HSP70, Annexin, integrin, and CD63. (E and F) PKH26-labeled IR+EV_{HM} was detected in the H9C2 cells (E) and heart tissue after leg vein injection (F); white arrows, PKH26. EV, extracellular vesicle; MSC, mesenchymal stem cell; IR, ischemia/reperfusion; EV_{HM}, hypoxia-preconditioned extracellular vesicles.

https://doi.org/10.3349/ymj.2018.59.6.736

(Invitrogen, Carlsbad, CA, USA) as per the manufacturer's instructions. After transfection for the indicated time periods, cells were analyzed for proliferation, and formaldehyde-fixed cells were obtained for immunofluorescence analysis.[19]

Immunofluorescence staining

Cells from the control and experimental groups were grown on general cell culture dishes and a flexible energy harvester, respectively. The cultured cells were fixed with 4% ice-cold formaldehyde (pH 7.2–7.3) for 1 h at room temperature, and then washed and permeated with 0.3% Triton X-100 for 30 min. Cells were washed and blocked with 5% bovine serum albumin (BSA) and 0.3% Triton X-100 in PBS for 30 min. Cells were washed and stained with GSK3β (Santa Cruz Biotechnology) and phosphor β-catenin (Santa Cruz Biotechnology) primary antibodies using 1% BSA with 0.3% Triton X-100 in PBS overnight in a cold room at 4°C. Cells were washed and stained with Alexa Fluor 488 and Alexa 555 secondary antibodies using 1% BSA with 0.3% Triton X-100 in PBS for 3 h at room temperature. Cells were washed three times for 5 min, and then stained with 4',6-diamidino-2-phenylindole (DAPI) during the final wash. Fluorescence images were recorded using a confocal microscope.

Statistical analysis

Data are presented as the mean±SEM. Patch clamp data were analyzed using pClamp software, version 10.4 (Axon Instruments, Foster City, CA, USA) and Origin Pro, version 9.0 (OriginLab Corp., Northampton, MA, USA). The parameters indicated under the different S1–S2 intervals, and multiple comparisons were determined by ANOVA analysis with Bonferroni post-hoc analyses. A value of $p<0.05$ was considered statistically significant. Details of materials and experimental procedures are available in Supplementary Materials and Methods (only online).

RESULTS

Confirmation of EV characteristics and transfer to cardiomyoblasts

Fifteen milliliters of each human MSC culture was pelleted at 300×g for 10 min to remove dead cells. Next, supernatants from both cell cultures were obtained by centrifugation at 750×g for 5 min and then at 1500×g for 15 min to remove large debris and apoptotic bodies, respectively. EVs from supernatants were

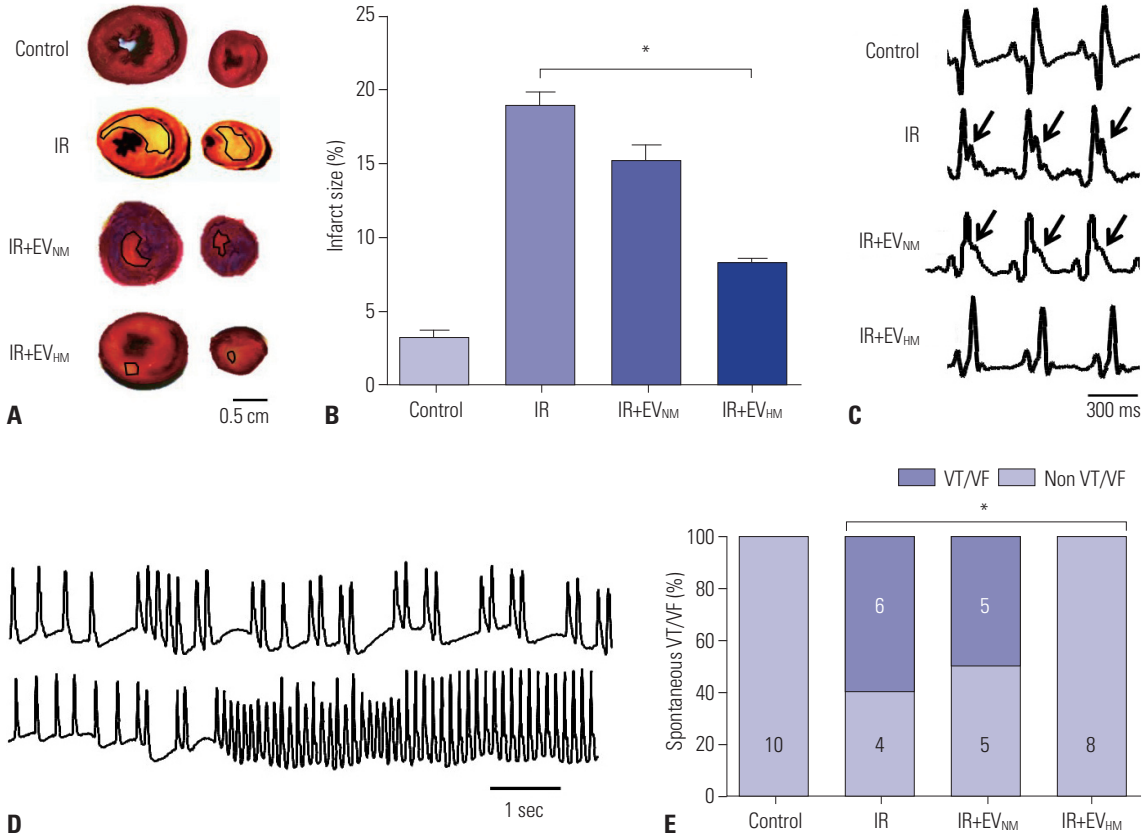

Fig. 2. Systemic injection of EV_{HM} decreases IR injury and arrhythmias in a rat IR injury model. (A and B) Comparison of 2,3,5-triphenyltetrazolium chloride (TTC) staining and reduction in the infarct size by the EVs (n=6 per group). (C) Typical examples of an EKG in the IR (n=10) and IR+EV (n=8) groups. (D) Typical examples of VT and VF in the IR group (n=10). (E) Comparison of spontaneous VT or VF. All data are presented as the mean±SEM; *$p<0.001$. EV, extracellular vesicle; IR, ischemia/reperfusion; VT, ventricular tachycardia; VF, ventricular fibrillation; EV_{HM}, hypoxia-preconditioned extracellular vesicles; EV_{NM}, normoxia-preconditioned extracellular vesicles.

pelleted and washed 3 times (45 min at 14000×g, room temperature) (Fig. 1A).

We confirmed the diameter of isolated EVs were <1000 nm using transmission electron microscopy (Fig. 1B) and nanoparticle tracking analysis (Fig. 1C). EVs were electrophoresed and analyzed by Western blotting using anti CD81, Hsp70, Annexin, integrin, and CD63 antibodies (Fig. 1D). PKH26-labeled IR+EV_{HM} was detected in H9C2 cells and heart tissue after leg vein injection (Fig. 1E and F).

EV_{HM} attenuated IR injury and arrhythmias in IR-injured rats

Fig. 2A shows the extent of the infarct size assessed by histology with TTC staining. Compared with the IR group (19±1%), the degree of infarct expansion was markedly decreased to a third in the IR+EV_{HM} group (7±2%, p<0.001) (Fig. 2B). The typical ST-segment elevation after IR injury was not observed in the IR+EV_{HM} group (Fig. 2C). Fig. 2D shows examples of ventricular tachycardia (VT) and ventricular fibrillation (VF) recorded by ambulatory Holter monitoring in the IR group. While spontaneous VT or VF was not observed in control rats, they were observed in six (60%) rats in the IR group (p=0.003). However, the VT episodes were not observed after systemic EV_{HM} treatment in the IR group (p<0.001) (Fig. 2E).

Fig. 3A and B show traces of action potentials (APs) and the typical maps of activation and AP duration (APD) at a pacing cycle length (CL) of 300 ms. In the IR group, the amplitude of APD of border (②) and infarcted zone (③) were noticeably improved, and activation was hindered. However, the amplitude of APD in the IR-injured zone was significantly restored, and activation was spread wider inside the infarcted zone in the IR+EV_{HM} group. The EV_{HM} treatment reversed IR-induced APD shortening. Fig. 3C show representative examples of conduction velocity (CV) maps for all four groups, and the EV_{HM} treatment generally recovered the IR-induced reduction of CV. The average CV was calculated from the vector maps at infarcted border zone or at corresponding sites.

Conduction velocity was considerably slowed, and the slope of the CV restitution curve became steeper after IR. In the IR+EV_{HM} group, the CV value and CV restitution slope were comparable to those of the control group. EV_{HM} significantly reduced the induction rate of VT/VF in the IR injury group (67% vs. 0%, p<0.05) (Supplementary Fig. 3, only online).

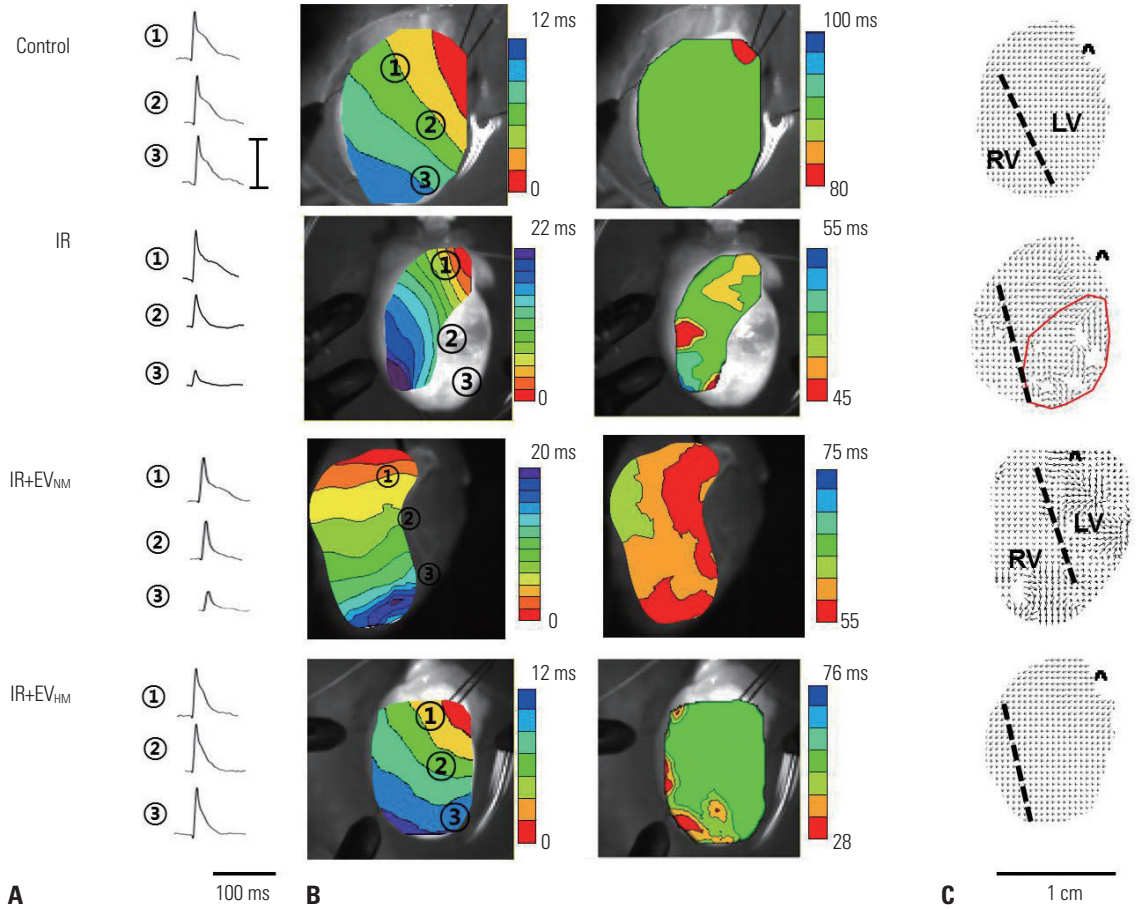

Fig. 3. Electrophysiologic effects of EV_{HM} after IR injury. (A) Sample traces of V_m from the three groups (cycle length=300 ms). (B) Representative activation (left panels) and action potential duration maps (right panels) from the three groups. (C) Conduction velocity vector maps. EV_{HM}, hypoxia-preconditioned extracellular vesicles; EV_{NM}, normoxia-preconditioned extracellular vesicles; IR, ischemia/reperfusion; LV, left ventricle, RV, right ventricle.

https://doi.org/10.3349/ymj.2018.59.6.736

Table 1. Effect of Extracellular Vesicles (EVs) on the Time Properties of the I_{Na} Current Recorded in Adult Rat Cardiomyocytes

	Maximum I_{Na} density (pA/pF)	E_{rev} (mV)	τ_{act} (ms)	τ_{inact} (ms)
Control (n=5)	-72.7±1.7	-35.8±3.7	0.7±0.1	8.1±0.8
IR (n=5)	-30.7±2.1*	-32.5±1.6	0.5±0.2	12.3±0.2*
IR+EV_{HM} (n=5)	-80.3±6.7	-40.0±1.7	0.6±0.2	8.7±0.5

IR, ischemia/reperfusion; EV_{HM}, hypoxia-preconditioned extracellular vesicles.
IR indicates hypoxia/reoxygenation.
*p<0.01. IR vs. IR+EV_{HM}.

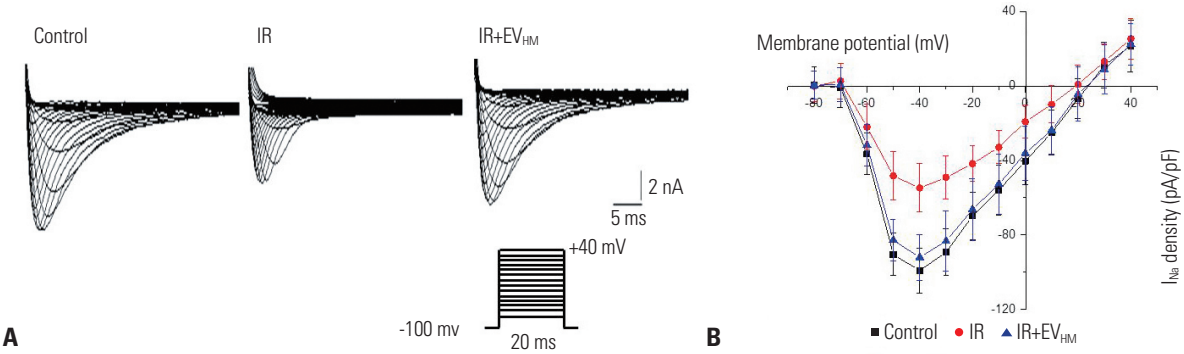

Fig. 4. EV_{HM} recovers the sodium current (I_{Na}) after IR injury. Representative traces of whole-cell currents recorded from adult rat cardiomyocytes during the control, IR, and IR+EV_{HM} conditions (A). Current/voltage relationship of I_{Na} under the three conditions (B). The protocol is indicated in the inset, and the number of cells recorded was five in each group. EV_{HM}, hypoxia-preconditioned extracellular vesicles; IR, ischemia/reperfusion.

Reversal of the sodium current (I_{Na}) reduced by hypoxic injury

To determine whether EV_{HM} directly alters the function of the cardiac sodium channel, I_{Na} was recorded in adult rat cardiomyocytes of the control (n=5), IR (n=5), and IR+EV_{HM} groups (n=5). As detailed in Table 1, compared with that recorded in the control cells (-73±2 pA/pF), the I_{Na} peak density was markedly decreased in the IR cells (-31±2 pA/pF, p=0.001), but not after EV_{HM} treatment (-80±7 pA/pF, p=0.002). The inactivation kinetics (τ_{inact}) were increased in the IR group (8±1 ms vs. 12±0.2 ms, p=0.001), but preserved in the IR+ EV_{HM} group (9±0.5 ms, p=0.001) (Fig. 4).

Since it is known that arrhythmia is particularly associated with gap junctions, we further examined the effects of EV_{HM} on the levels of the gap junction protein Cx43. Whereas Cx43 (brown color, arrows) was sufficient at the cell-cell junctions in normal myocardium, Cx43 expression was decreased in IR myocardium. Injection of EV_{HM} resulted in the reorganization of Cx43 at the cell-cell junction (Supplementary Fig. 4A, only online). According to Western blot assay of Cx43, IR-induced reduction of Cx43 (0.2-fold from normal) was recovered to 0.5-fold to normal level by EV_{HM} treatment (Supplementary Fig. 4B, only online). This result shows that EV_{HM} changed the gap junction that was interrupted by IR injury, and then leading to stable conduction.

Effects of EV on the Wnt signaling pathway

GSK-3β is associated with the Wnt-Fizzled pathway, and Wnt signaling is most well known to be a significant modulator of Cx43-dependent intercellular coupling in the heart.[20] Thus, the level of Wnt signaling proteins were further assayed (Fig. 5A).

After IR injury, compared with control, p-β-catenin/β-catenin increased by 2.6-fold (p<0.001), and p-GSK3β/GSK3β was decreased by 0.7-fold (p=0.036). Compared to IR, EV_{HM} treatment decreased p-β-catenin/β-catenin by 0.4-fold (p=0.004), and increased p-GSK3β/GSK3β by 1.4-fold (p=0.032) and Wnt1 by 1.3-fold (p<0.001) (Fig. 5B).

The putative target prediction of validated miRNAs by qRT-PCR was performed using TargetScan (Version 6.2) and mirDB, providing an individual miRNA repression rate for target genes related with Wnt pathway. Combining this p-value and its abundance value for each miRNA, the repression rates for the whole miRNA profile were calculated. Based on the results, the significantly expressed five miRNAs were selected. To evaluate the change in miRNAs related with Wnt pathway after IR injury and EV_{HM} treatment, we next performed qRT-PCR of miR-26, miR-148a, miR-31, miR-27a, miR-200a, and miR-34b in hearts from each study group. We found that miR-26a was significantly deceased in the IR model and reversed after EV_{HM} treatment (Fig. 5C).

Cardioprotection effect of EV_{HM} via miRNA26a

It is widely known that upregulation of GSK3β and p-β-catenin is closely associated with IR injury. Fig. 6A shows confocal microscope images of H9C2 cells upon immunofluorescence staining for GSK3β and p-β-catenin. In hypoxic conditions, both GSK3β (3.1-fold) and p-β-catenin (3.8-fold) increased; however, EV_{HM} and miR-26 effectively prevented increases in GSK3β (1.2-fold, p<0.001 vs. IR group) and p-β-catenin (1.1-fold, p<0.001 vs. IR group) in hypoxic conditions. After suppression

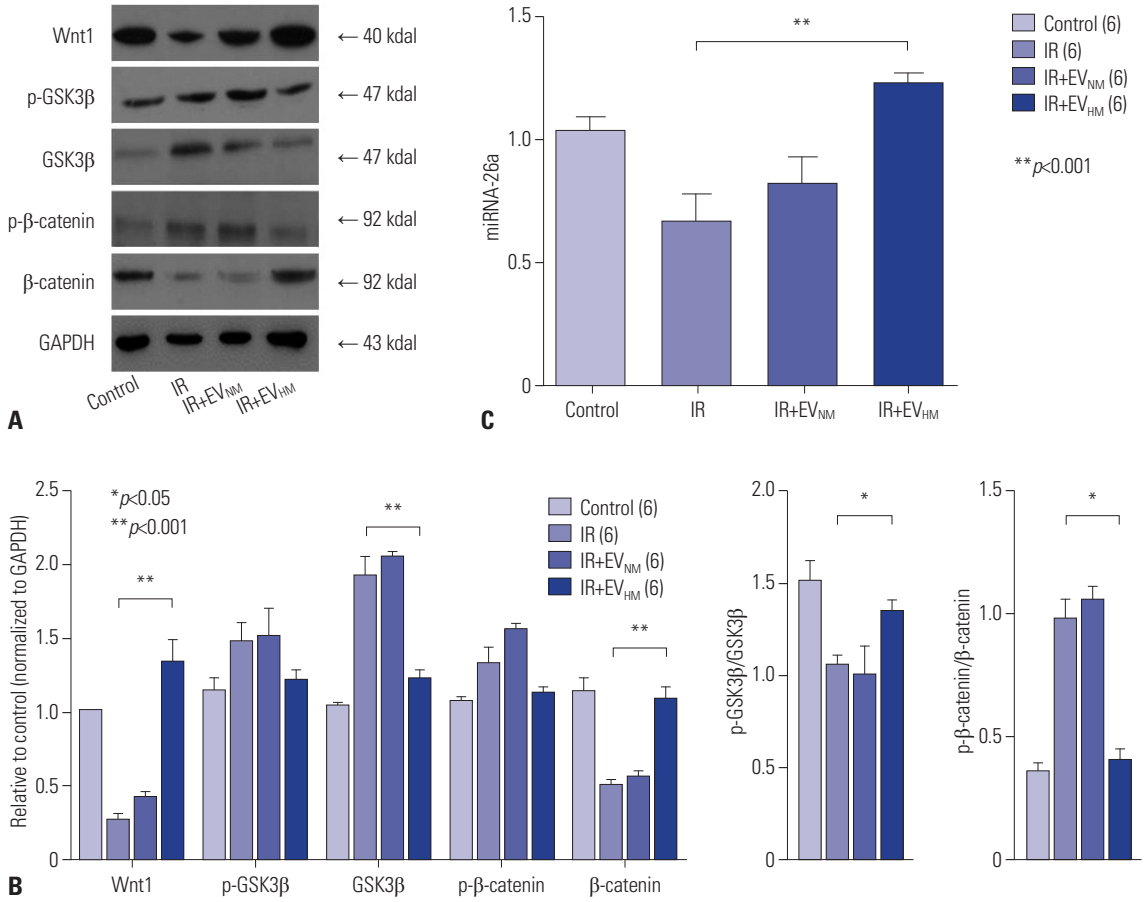

Fig. 5. EVs decrease and increase Wnt signaling proteins after IR injury and elevation of miRNA-26a in EV_{HM} and the reversal of miRNA-26a by EV_{HM} after IR injury. (A and B) Expression level of Wnt signaling proteins (e.g., Wnt1, GSK3β, p-GSK3β, β-catenin, and p-β-catenin) (n=6 per group). All data are presented as the mean±SEM; *p<0.05, **p<0.001. (C) Reversal of miRNA-26a after IR injury by EV_{HM} (n=6 per group). Data are presented as the mean±SEM; **p<0.001. EV, extracellular vesicle; EV_{HM}, hypoxia-preconditioned extracellular vesicles; EV_{NM}, normoxia-preconditioned extracellular vesicles; IR, ischemia/reperfusion.

of miR-26a using anti-miR-26a, the effect of EV_{HM} was eliminated; EV_{HM} showed no effect on GSK3β and p-β-catenin (Fig. 6B). The effects of miR-26a and anti-miR-26a on different conditions are presented in Supplementary Fig. 5 (only online).

DISCUSSION

The main findings of this study were that EVs derived from hypoxia-preconditioned MSCs attenuated IR injury by suppressing GSK3β expression. Moreover, they increased electrical conduction and Cx43 expression by increasing Wnt1. Finally, miR-26a was increased in EVs after hypoxic stress, and was related with decreases in GSK3β and p-β-catenin. These findings highlight a potential new beneficial tool in IR injury.

Systemic injection of EVs protects the heart against IR injury

In this study, the degree of infarct expansion was markedly decreased by the systemic injection of EVs originating from hypoxic human MSCs. EV_{HM} effectively attenuated increases in GSK3β, which is important in the process of IR injury. During ischemic preconditioning (IPC), GSK3β is phosphorylated and inhibited in a Wortmannin-sensitive manner.[21] GSK-3β is inactivated by phosphorylation. Akt, PKC, and PKA phosphorylate and inactivate GSK3β. FrzA, a secreted antagonist of the Wnt/Frizzled pathway, decreases the phosphorylation of GSK3β, independent of Akt activity. Overexpression of FrzA blocks the IPC-mediated increase in phosphorylation of GSK3β and blocks the protection afforded by IPC.[22] Phosphorylation and inactivation of GSK3β are antiapoptotic. Tong, et al.[23] showed that preconditioning results in increased phosphorylation of GSK3β, which is blocked by inhibitors of PI3K. In this study, EV_{HM} reduced the sizes of infarct areas. We also confirmed that EV_{HM} was well delivered to the infarct border zone. Therefore, EV functions as a miRNA source to the cell of the infarct border zone.

EV_{HM} improves electrical conduction

Cells in the surviving peri-infarct zone have prepotentials and notches on phase 0 upstrokes, decreased space constants, and

https://doi.org/10.3349/ymj.2018.59.6.736

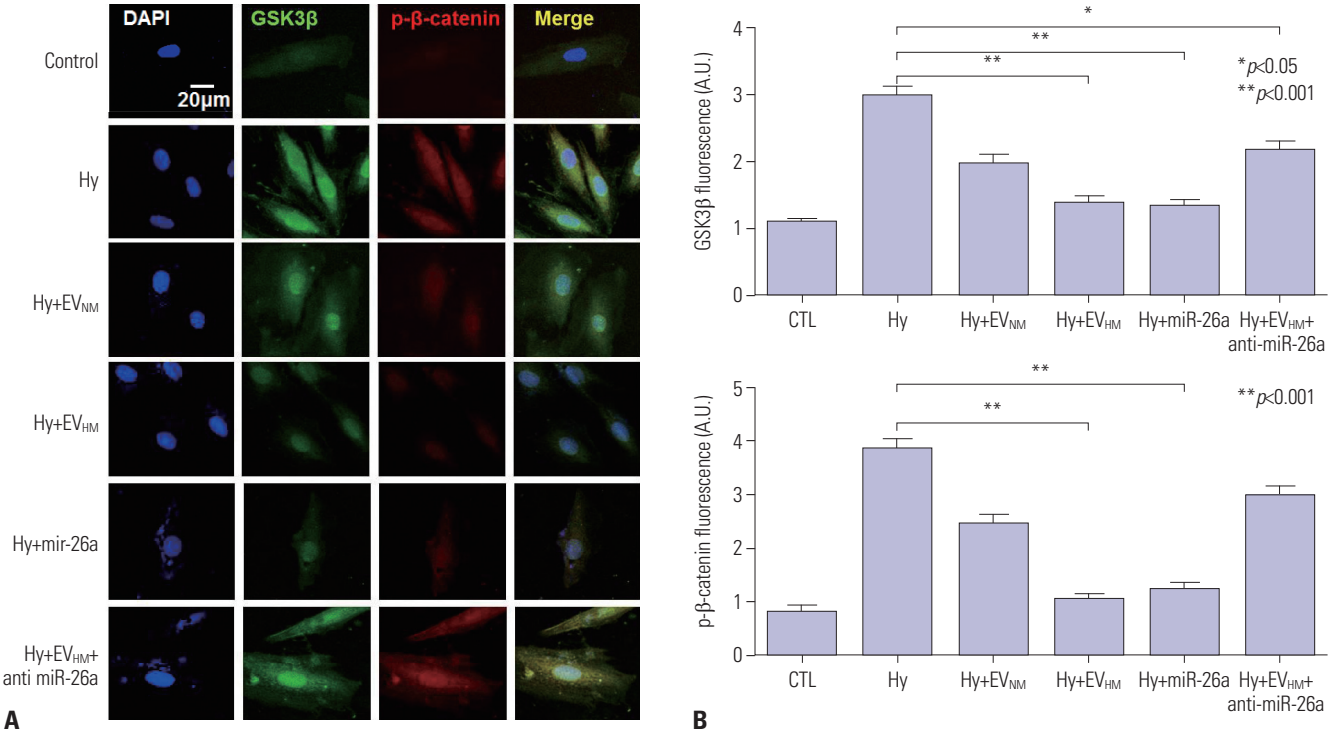

Fig. 6. Confocal microscope image of H9C2 cells showing GSK3β and p-β-catenin staining in various conditions. (A) Hypoxia-preconditioned extracellular vesicles (EV_{HM}), compared with EV_{NM} (normoxic), significantly prevented ischemia/reperfusion injury-induced increases in GSK3β and decreases in p-β-catenin. These effects were abrogated by anti-miRNA-26a. (B) Quantitative analysis of fluorescence signals in H9C2 cells stained for GSK3β and p-β-catenin.

discontinuous propagation due to abnormal cell-to-cell coupling.[24] Surviving border-zone tissue exhibits a decreased phase amplitude and upstroke velocity (dV/dtmax), reminiscent of a reduced I_{Na}.[25] Isolated border zone cardiomyocytes also have a reduced dV/dtmax[26] and marked irregularities in the I_{Na}, including a diminished current density, increased inactivation, and slowed reactivation.[27] Marked alterations in the gap junction organization and Cx43 distribution happen within improved myocardial infarctions.[28] Thus, coupling irregularities due to Cx43 changes are central to ventricular arrhythmogenesis after infarction. This study showed that EVs improve Na^+ current and Cx43 expression, which were decreased after IR injury. GSK3β is associated with the Wnt-Fizzled pathway, and Wnt signaling is best known to be a significant modulator of Cx43-dependent intercellular coupling in the heart.[20] Consistently, Wnt 1 was significantly increased with EV_{HM} in the IR injury model.

EV_{HM} had a cardioprotective effect after IR injury via miRNA-26a

EVs can directly interact with the ligands present on the surface of target cells and activate cascade signaling. In addition, EVs can transfer proteins, mRNA, microRNA, and bioactive lipids by interacting with target cells by either fusion or internalization.[29,30] Numerous miRNAs have been found to regulate regeneration and cardiac repair,[31] and these microparticles have also been identified as immature mRNA when secreted from MSCs.[32] The IR injury protective effect of EVs might be mediated by heat-shock proteins or a specific microRNA. It is noteworthy that heat shock protein 20, compared with other small heat-shock proteins, is mostly upregulated in animal hearts during ischemic conditions.[33] Increased miRNA-494 levels protect hearts against IR injury.[34]

Icli, et al.[35] reported that miR-26a acts as a previously unrecognized pivotal regulator of pathological and physiological angiogenesis by targeting a SMAD1-Id1-p21WAF/CIP1/p27 signaling axis to promote an antiangiogenic program in ECs. Furthermore, neutralization of miR-26a was found to rapidly induce angiogenesis, to reduce acute myocardial infarction (MI) size, and to improve heart function in mice. However, an acute IR model demonstrated an essential role for miR-26a in inhibiting high mobility group box-1 (HMGB1) expression and attenuating cardiac IR injury. miR-26a overexpression results in reduced cardiac IR injury and suppressed HMGB1 expression. Therefore, the discrepancy of the effect of miR-26 might be related with the stage of MI or model of MI.

GSK-3β is a key integration point in IPC, with GSK-3β phosphorylation/inhibition raising the threshold for oxidative stress-induced mitochondrial permeability transition, and thereby protecting the heart.[36] Many other studies have reported that the inhibition of GSK-3β mimics the effect of IPC and reduces infarct size in rats.[21,37] In contrast, diabetic rat hearts show increased GSK-3β activity and reduced cardioprotection from IPC.[38] In this

study, GSK-3β phosphorylation/inhibition of IR+EV_{HM} model could explain the reduced infarct size of EV_{HM}. Consistent with our report, Suh, et al.[39] reported that up-regulation of miR-26a repress GSK-3β protein expression.

This study showed that increased miR-26a levels in EV_{HM} protected hearts after IR injury. We also demonstrated that EV_{HM} directly targets GSK3β using anti-miR-26a. The involvement of miR-26a in the suppression of GSK3β after IR injury was supported by the experiment showing that suppression of GSK3β by EV_{HM} is eliminated by the transfection of anti-miR-26a. miR-26a was significantly deceased in the IR model and reversed after EV_{HM} treatment. However, the delivery of miR-26 by EV_{HM} was not evaluated in this study. In H9C2 cells, EV_{NM} also had a protective effect without statistical significance. Inhibition with anti-miR-26a decreased effect of Hy+EV_{HM} to the same level as Hy+EV_{NM}. Therefore, the protective effect of EV_{NM} might be miR-26a-independent. Moreover, the transfection of miR-26a successfully suppressed GSK3β in H9C2 cells after hypoxic stress.

There are some limitations to our research. The proteins of the EVs were not assayed in this study. Kim, et al.[40] profiled the MSC-EV proteome to investigate their therapeutic effects, and identified 730 EV proteins. A functional enrichment analysis showed that cellular processes represented by the MSC-EV proteins include cell proliferation, adhesion, migration, and morphogenesis. Therefore, the antiarrhythmic effects are related to the combined effects of several EV proteins. This study could not demonstrate whether miR-26a targets GSK3β directly. Dual luciferase assay should be carried out for the evaluation of miRNA binding on 3'UTR of GSK3β. Future studies are needed to reveal the detailed mechanism.

In summary, our study demonstrates that EV_{HM} reduced IR injury by suppressing GSK3β expression and increased Cx43 expression suggesting that the beneficial effect of EV_{HM} is related with Wnt signaling pathway. These effects might be correlated with miR-26a. These findings highlight a potential new beneficial tool in IR injury. Further study is need to reveal whether EV-derived miR-26 actually affects the function of the gap junction (or at least the amount of Cx43).

ACKNOWLEDGEMENTS

This study was supported by research grants from the Basic Science Research Program through the National Research Foundation of Korea funded by the Ministry of Education, Science and Technology (NRF-2017R1A2B3003303), and from the Korean Healthcare Technology R&D project funded by the Ministry of Health & Welfare (HI16C0058).

ORCID

Hyewon Park https://orcid.org/0000-0003-2573-4951
Boyoung Joung https://orcid.org/0000-0001-9036-7225

REFERENCES

1. Maroko PR, Kjekshus JK, Sobel BE, Watanabe T, Covell JW, Ross J Jr, et al. Factors influencing infarct size following experimental coronary artery occlusions. Circulation 1971;43:67-82.
2. Reimer KA, Lowe JE, Rasmussen MM, Jennings RB. The wavefront phenomenon of ischemic cell death. 1. Myocardial infarct size vs duration of coronary occlusion in dogs. Circulation 1977;56:786-94.
3. Bolli R, Becker L, Gross G, Mentzer R Jr, Balshaw D, Lathrop DA; NHLBI Working Group on the Translation of Therapies for Protecting the Heart from Ischemia. Myocardial protection at a crossroads: the need for translation into clinical therapy. Circ Res 2004;95:125-34.
4. Mathivanan S, Ji H, Simpson RJ. Exosomes: extracellular organelles important in intercellular communication. J Proteomics 2010; 73:1907-20.
5. Yellon DM, Davidson SM. Exosomes: nanoparticles involved in cardioprotection? Circ Res 2014;114:325-32.
6. Raposo G, Stoorvogel W. Extracellular vesicles: exosomes, microvesicles, and friends. J Cell Biol 2013;200:373-83.
7. Ratajczak J, Miekus K, Kucia M, Zhang J, Reca R, Dvorak P, et al. Embryonic stem cell-derived microvesicles reprogram hematopoietic progenitors: evidence for horizontal transfer of mRNA and protein delivery. Leukemia 2006;20:847-56.
8. Hunter MP, Ismail N, Zhang X, Aguda BD, Lee EJ, Yu L, et al. Detection of microRNA expression in human peripheral blood microvesicles. PLoS One 2008;3:e3694.
9. Aliotta JM, Pereira M, Johnson KW, de Paz N, Dooner MS, Puente N, et al. Microvesicle entry into marrow cells mediates tissue-specific changes in mRNA by direct delivery of mRNA and induction of transcription. Exp Hematol 2010;38:233-45.
10. Sahoo S, Klychko E, Thorne T, Misener S, Schultz KM, Millay M, et al. Exosomes from human CD34(+) stem cells mediate their proangiogenic paracrine activity. Circ Res 2011;109:724-8.
11. Lai RC, Arslan F, Lee MM, Sze NS, Choo A, Chen TS, et al. Exosome secreted by MSC reduces myocardial ischemia/reperfusion injury. Stem Cell Res 2010;4:214-22.
12. Choi M, Ban T, Rhim T. Therapeutic use of stem cell transplantation for cell replacement or cytoprotective effect of microvesicle released from mesenchymal stem cell. Mol Cells 2014;37:133-9.
13. Beninson LA, Fleshner M. Exosomes: an emerging factor in stress-induced immunomodulation. Semin Immunol 2014;26:394-401.
14. Baixauli F, Lopez-Otin C, Mittelbrunn M. Exosomes and autophagy: coordinated mechanisms for the maintenance of cellular fitness. Front Immunol 2014;5:403.
15. Gnecchi M, He H, Liang OD, Melo LG, Morello F, Mu H, et al. Paracrine action accounts for marked protection of ischemic heart by Akt-modified mesenchymal stem cells. Nat Med 2005;11:367-8.
16. Takahashi M, Li TS, Suzuki R, Kobayashi T, Ito H, Ikeda Y, et al. Cytokines produced by bone marrow cells can contribute to functional improvement of the infarcted heart by protecting cardiomyocytes from ischemic injury. Am J Physiol Heart Circ Physiol 2006; 291:H886-93.
17. Arslan F, Lai RC, Smeets MB, Akeroyd L, Choo A, Aguor EN, et al. Mesenchymal stem cell-derived exosomes increase ATP levels, decrease oxidative stress and activate PI3K/Akt pathway to enhance myocardial viability and prevent adverse remodeling after myocardial ischemia/reperfusion injury. Stem Cell Res 2013;10:301-12.
18. Park H, Ku SH, Park H, Hong J, Kim D, Choi BR, et al. RAGE siRNA-mediated gene silencing provides cardioprotection against ventricular arrhythmias in acute ischemia and reperfusion. J Control Release 2015;217:315-26.

https://doi.org/10.3349/ymj.2018.59.6.736

19. Zhang J, Han C, Wu T. MicroRNA-26a promotes cholangiocarcinoma growth by activating β-catenin. Gastroenterology 2012;143:246-56.e8.
20. Ai Z, Fischer A, Spray DC, Brown AM, Fishman GI. Wnt-1 regulation of connexin43 in cardiac myocytes. J Clin Invest 2000;105:161-71.
21. Tong H, Imahashi K, Steenbergen C, Murphy E. Phosphorylation of glycogen synthase kinase-3beta during preconditioning through a phosphatidylinositol-3-kinase--dependent pathway is cardioprotective. Circ Res 2002;90:377-9.
22. Barandon L, Dufourcq P, Costet P, Moreau C, Allieres C, Daret D, et al. Involvement of FrzA/sFRP-1 and the Wnt/frizzled pathway in ischemic preconditioning. Circ Res 2005;96:1299-306.
23. Tong H, Chen W, Steenbergen C, Murphy E. Ischemic preconditioning activates phosphatidylinositol-3-kinase upstream of protein kinase C. Circ Res 2000;87:309-15.
24. Gardner PI, Ursell PC, Fenoglio JJ Jr, Wit AL. Electrophysiologic and anatomic basis for fractionated electrograms recorded from healed myocardial infarcts. Circulation 1985;72:596-611.
25. Nattel S, Maguy A, Le Bouter S, Yeh YH. Arrhythmogenic ion-channel remodeling in the heart: heart failure, myocardial infarction, and atrial fibrillation. Physiol Rev 2007;87:425-56.
26. Lue WM, Boyden PA. Abnormal electrical properties of myocytes from chronically infarcted canine heart. Alterations in Vmax and the transient outward current. Circulation 1992;85:1175-88.
27. Pu J, Boyden PA. Alterations of Na+ currents in myocytes from epicardial border zone of the infarcted heart. A possible ionic mechanism for reduced excitability and postrepolarization refractoriness. Circ Res 1997;81:110-9.
28. Matsushita T, Takamatsu T. Ischaemia-induced temporal expression of connexin43 in rat heart. Virchows Arch 1997;431:453-8.
29. van der Vlist EJ, Nolte-'t Hoen EN, Stoorvogel W, Arkesteijn GJ, Wauben MH. Fluorescent labeling of nano-sized vesicles released by cells and subsequent quantitative and qualitative analysis by high-resolution flow cytometry. Nat Protoc 2012;7:1311-26.
30. Martinez MC, Tual-Chalot S, Leonetti D, Andriantsitohaina R. Microparticles: targets and tools in cardiovascular disease. Trends Pharmacol Sci 2011;32:659-65.
31. Wen Z, Zheng S, Zhou C, Yuan W, Wang J, Wang T. Bone marrow mesenchymal stem cells for post-myocardial infarction cardiac repair: microRNAs as novel regulators. J Cell Mol Med 2012;16:657-71.
32. Chen TS, Lai RC, Lee MM, Choo AB, Lee CN, Lim SK. Mesenchymal stem cell secretes microparticles enriched in pre-microRNAs. Nucleic Acids Res 2010 ;38:215-24.
33. De Celle T, Vanrobaeys F, Lijnen P, Blankesteijn WM, Heeneman S, Van Beeumen J, et al. Alterations in mouse cardiac proteome after in vivo myocardial infarction: permanent ischaemia versus ischaemia-reperfusion. Exp Physiol 2005;90:593-606.
34. Wang X, Zhang X, Ren XP, Chen J, Liu H, Yang J, et al. MicroRNA-494 targeting both proapoptotic and antiapoptotic proteins protects against ischemia/reperfusion-induced cardiac injury. Circulation 2010;122:1308-18.
35. Icli B, Wara AK, Moslehi J, Sun X, Plovie E, Cahill M, et al. MicroRNA-26a regulates pathological and physiological angiogenesis by targeting BMP/SMAD1 signaling. Circ Res 2013;113:1231-41.
36. Juhaszova M, Zorov DB, Kim SH, Pepe S, Fu Q, Fishbein KW, et al. Glycogen synthase kinase-3beta mediates convergence of protection signaling to inhibit the mitochondrial permeability transition pore. J Clin Invest 2004;113:1535-49.
37. Fukumoto S, Hsieh CM, Maemura K, Layne MD, Yet SF, Lee KH, et al. Akt participation in the Wnt signaling pathway through Dishevelled. J Biol Chem 2001;276:17479-83.
38. Yadav HN, Singh M, Sharma PL. Involvement of GSK-3β in attenuation of the cardioprotective effect of ischemic preconditioning in diabetic rat heart. Mol Cell Biochem 2010;343:75-81.
39. Suh JH, Choi E, Cha MJ, Song BW, Ham O, Lee SY, et al. Up-regulation of miR-26a promotes apoptosis of hypoxic rat neonatal cardiomyocytes by repressing GSK-3β protein expression. Biochem Biophys Res Commun 2012;423:404-10.
40. Kim HS, Choi DY, Yun SJ, Choi SM, Kang JW, Jung JW, et al. Proteomic analysis of microvesicles derived from human mesenchymal stem cells. J Proteome Res 2012;11:839-49.